RESEARCH ARTICLE

Establishment and Evaluation of a Rat Model of Medial Malleolar Fracture with Vascular Injury

Jinglai Sun, MBS[1,2], Qifeng Li, PhD[1], Shuo Wang, MBS[1,3], Guangpu Wang, MBS[1,2], Jing Zhao, MBS[1,2], Huanming Li, MM[2,4], Chong Liu, MM[2,5,6], Yifan Shi, BM[7], Zhigang Li, MM[2,8] 🔘, Hui Yu, MD, PhD[1,2,3]

[1]Department of Biomedical Engineering, Tianjin Key Laboratory of Biomedical Detecting Techniques and Instruments, [2]Tianjin Joint Laboratory of Intelligent Medicine, Tianjin 4TH Centre Hospital and [3]Academy of Medical Engineering and Translation Medicine, Tianjin University and Department of [4]Cardiovascular, [5]Central Laboratory, [6]Anesthesiology, [7]Imaging and [8]Emergency Medicine, Tianjin 4TH Centre Hospital, Tianjin, China

Objective: A stable animal model was needed to study bone non-union caused by insufficient blood supply, the main object of this paper is to develop a medial malleolar fracture model with controllable arterial vascular injuries in rats for revealing the biochemical mechanism of non-union by insufficient blood supply.

Methods: A total of 18 rats were randomly divided into three equal groups: the Sham group, the Fracture group, and the Fracture + Vascular group. The animals were subjected to unilateral medial malleolar bone fracture and vascular injury using customized molding equipment. The fracture site was scanned by micro-CT, and vascular injury was evaluated by laser Doppler flowmetry (LDF) 24 h after modeling. Histological examination (HE), alkaline phosphatase (ALP) and tartrate-resistant acid phosphatase (TRAP) staining, immunohistochemistry and immunofluorescence were conducted on the medial malleolar fracture tissues of three rats randomly selected from each group 24 h after modeling. Subsequently, to further confirm the success of fracture modeling, the fracture sites of three other rats in each group underwent micro-CT scanning again 6 weeks after surgery.

Results: The results of a 24 h micro-CT showed that all rats used to create the fracture models showed controlled injury of the medial malleolus. The model was stable, and the satisfaction of the homemade equipment agreed with the expectation. LDF showed that the blood flow of rats in the Fracture + Vascular group decreased significantly 24 h after fracture injury, while collateral blood flow perfusion increased by 50% on average. The results of HE, ALP and TRAP staining in the medial malleolus showed that the number of osteoblasts (OBs) and osteoclasts (OCs) in the Fracture group increased significantly, but the number of OBs and OCs in the Fracture + Vascular group decreased sharply relative to the number in the Sham group 24 h later. Furthermore, immunohistochemistry and immunofluorescence results showed that the number of neovessels in the Fracture group was significantly increased, while the number of neovessels in the Fracture + Vascular group was significantly decreased, which was consistent with the above results. After 6 weeks of modeling, the micro-CT results showed that the fractures in the Fracture group had healed substantially, while those in the Fracture + Vascular group had not.

Conclusion: This study provided a reproducible and stable experimental animal model for medial malleolar fractures with arterial injury.

Key words: Animal model; Ankle; Arterial vascular; Fracture; Rat

Introduction

Ankle fracture is a common clinical form of fracture injury.[1,2] According to the literature, non-union or delayed bone union after fracture is a common complication in orthopedics, with the rate of non-union reaching 21%.[3] Non-union can be divided into avascular or atrophic and hypervascular or hypertrophic non-unions.[4] Existing studies have shown that atrophic non-union is mainly caused by poor blood supply,[5] bone loss and periosteal injury, hypertrophic non-union is mainly caused by poor fixation. However the pathogenesis of atrophic non-union is still unclear. The progression toward successful prevention and treatment of non-union is impeded by the lack of available preclinical animal models, which is indispensable for revealing biochemical mechanism and evaluating the efficacy of therapeutic treatments.

During the past decades, there have been some reports on non-union models. In 2021, Wu et al.[6] reported a tibial hypertrophic non-union model with relative movement of fracture end 15 weeks later. In 2002, Park et al.[7-9] reported a construction of a fracture non-union model by multiple surgical cleaning of the broken end of the fracture. In 2008, Kaspar et al.[10-12] reported a model of atrophic fracture non-union was successfully constructed by periostectomy, curettage of medullary cavity, burning of broken end and external fixation. After 8 weeks, histological and imaging examination showed that the model was successfully constructed. These models focused on fracture and ligament injury and does not consider the effect of vascular injury on fracture non-union.[13] Evidence indicates that the growth of blood vessels in bone and osteogenesis are coupled.[14] Good blood supply is the primary condition necessary to promote fracture healing.[15-17] The quality of the local blood supply leads to the differentiation of osteogenic cells. If the local blood supply is good, osteogenic cells differentiate into osteoblasts. However, if the local blood supply is poor, osteogenic cells will differentiate into chondroblasts.[18] Therefore, when a fracture is accompanied by vascular injury, both the formation of new blood vessels at the fracture site and the osteogenic process will be slow.[19] therefore, the establishment of a rapid, effective, repeatable and stable animal model of vascular injury fracture non-union is essential for revealing biochemical mechanism of blood supply in the process of fracture healing.

The goals of the present study were: (i) to develop a consistent and repeatable non-union model of ankle fracture in the most commonly used medical animal, the rat, for revealing biochemical mechanism of non-union; (ii) to explore the macroscopic and radiographic changes of the fractured medial malleolars in different groups as time progresses; and (iii) to preliminarily assess the effect of blood supply on rehabilitation of medial malleolus fracture.

Materials and Methods

Animals and Experimental Design

A total of 18 mature male Sprague–Dawley (SD) rats, with a median age of 55 days (range, 48–60 days) and a median body weight of 200 g (range, 180–210 g), were provided by Beijing Charles River Experimental Animal Technology Co., Ltd. All rats were reared in six approved cages in the experimental animal center of Tianjin 4th Centre Hospital, China. Pairs of rats were reared in one cage, and they had free access to food and water. The size of each cage was 470 mm × 300 mm × 150 mm, ensuring enough space to allow the rats to move freely. The rats were reared in a well-ventilated environment with room temperature maintained at 23–25 °C, humidity maintained at 50%–70%, and a light cycle that maintained a 12/12 h circadian rhythm. All animal experiments were approved by the experimental animal ethics committee of Tianjin University (No. TJUE-2021-137) and were conducted in strict accordance with the national regulations on experimental animal ethics.

The animals were fasted 24 h before surgery, which was performed in an aseptic animal operating room. The animals were randomly divided into three groups of six rats each. In the Sham group, the rats were subjected to only skin incision, and no fracture or vascular injury occurred. In the Fracture group, the depth of the fracture reached the trabecular bone, but the saphenous artery was not damaged. In the Fracture + Vascular group, the trabecular bone and saphenous artery were damaged. During the whole experiment, the room temperature was maintained at 37 °C, and the anal temperature was maintained at 37 °C. Three rats were reared in each cage after the operation, and they had free access to food and water. The animals and experimental design are shown in Fig. 1. After 24 h, all animals underwent micro-CT scanning and LDF detection. Three rats from each group were killed, and then the right distal tibia was sliced into paraffin sections for tissue staining. After 6 weeks, the remaining rats underwent micro-CT scanning.

Surgical Procedures

Before the surgical procedures, all the animals underwent X-ray evaluation to verify that the osteoepiphyseal lines of the ankle bone were not closed, ensuring that all animals were skeletally immature. The animals were fasted for 24 h before surgery, which was performed in an aseptic animal operating room. Before the operation, the rats in each cage were placed in an anesthesia induction box and preanesthetized with 2%–3% isoflurane gas (RWD R540 small animal anesthesia machine). After complete anesthesia, the rats were fixed in the supine position on the operating table and then fitted with a gas anesthesia breathing mask to maintain anesthesia. The skin, fascia, and muscle layers were separated, and the medial malleolus juncture was exposed (Fig. 2A). In the ankle structure diagram (Fig. 2B), the white arrow indicates the fracture site of the medial malleolus. The rat was fixed onto the molding instrument (Fig. 2C), and the right ankle
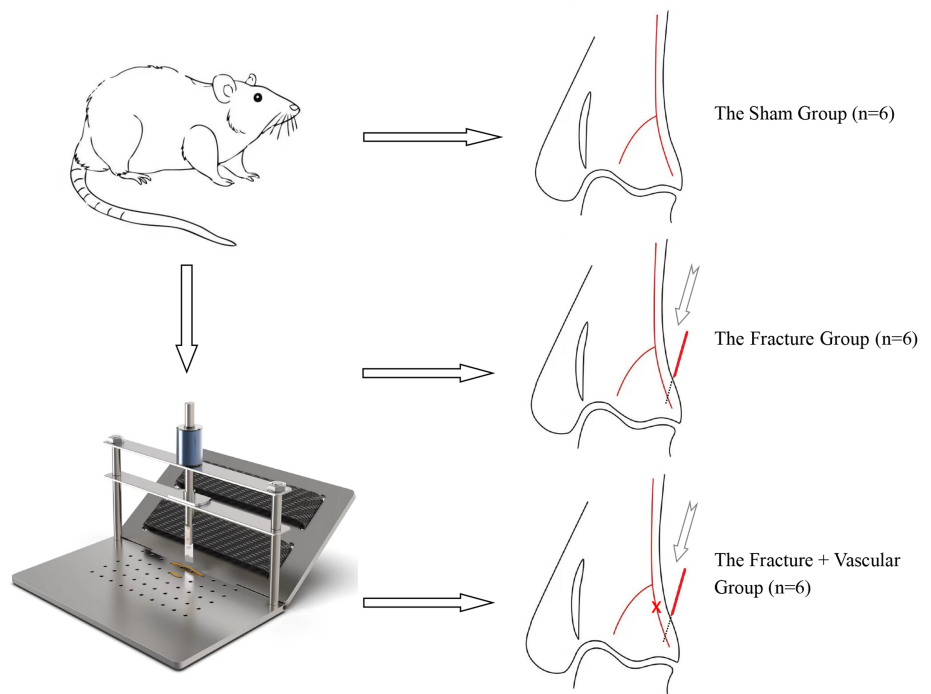
Fig. 1 Experimental flow chart. A total of 18 rats were equally divided into three groups. The Sham group ($n = 6$) underwent a sham surgical procedure, while the other two groups underwent modeled procedures, which attempted to simulate medial malleolar fracture, with (the Fracture + Vascular group, $n = 6$) or without vascular injuries (the Fracture group, $n = 6$). Besides intraoperative appearance and postoperative recovery, macroscopic and radiographic characteristics of the medial malleolars were recorded and assessed by a semi-quantitative scoring system at 24 h, 6 weeks, respectively.

was tightly enfolded by a customized plastic brace. The animal bed was adjusted to ensure that the osteotome of the molding equipment was at an angle of 37° from the centerline of the medial malleolus. While maintaining the operated limb at the correct position, a gravity-accelerated mass slid down from a 0.5 meter height along the slide rod and impacted the right medial malleolus. Cortical bone was broken under pressures above 133 MPa. The instrument used a 1 kg gravity-accelerated mass. A breach (2 mm wide) was cut from the inferomedial aspect of the ankle end toward the central medial malleolus (Fig. 2D). The molding instrument was customized by Tianjin Bai Wangda Science & Technology Co. Ltd., China. Moreover, the saphenous artery of the rats, shown by the white arrow (Fig. 2E), in the Fracture + Vascular group was cut off. The wound was sewn up after the operation (Fig. 2F). All rats were carefully protected during the operation.

Micro-CT Scanning
A total of 18 animals were subjected to micro-CT scanning using a Skyscan system (Bruker, Berlin, Germany), with scans performed after 24 h and 6 weeks at 85 kV, 200 μA, and a spatial resolution of 10 μm.

Laser Doppler Flowmetry (LDF) Scanning
The PeriCam PSI System® (Perimed AB, Järfälla, Sweden) is a blood perfusion imager 70 mW system based on Laser Speckle Contrast Analysis (LASCA) technology using a laser wavelength of 785 nm. The injury and reconstruction of blood vessels in the fracture site can be judged in the same area of interest by the amount of perfusion.

Histological Examination (HE)
The fixed ankle bones were decalcified in EDTA solution for 4–5 weeks and cut coronally into two equal parts. The specimens were dehydrated, embedded in paraffin, cut into 5 μm slices, and stained with HE. An area in the frontal plane of the ankle, which coincided with the ROI of the micro-CT scan, was selected as the ROI and examined under a light microscope (Olympus, Tokyo, Japan). Image-Pro Plus software (Silver Spring, Montgomery, MD, USA) was used to calculate the osteocyte count.

TRIP and ALP Examination
TRAP Staining
According to the package instructions of the TRAP staining solution, the experimenter prepared the TRAP incubation solution. The paraffin sections were dewaxed in water, and then the premixed TRAP staining solution was added and incubated at 37°C for 30 min. After cleaning with distilled water, 2-amino-2-methyl-1, 3-propane-diol (AMPD)-HCl (pH 9.4) solution was added to the slices for 10 min. Then, the paraffin sections were dyed again with methyl green and distilled water, dried and sealed. The field of view was selected using an inverted optical microscope (40×), and the images were collected and analyzed. The number of osteoclasts (OCs) per unit area of each TRAP staining scanning film was counted by ImageJ software. The experiment was repeated three times for each group, and the average value was taken. The cytoplasm of OC was wine red, and the nucleus was light green.

ALP Staining
The paraffin sections were dewaxed in water, and then the premixed ALP staining solution was added. The sections

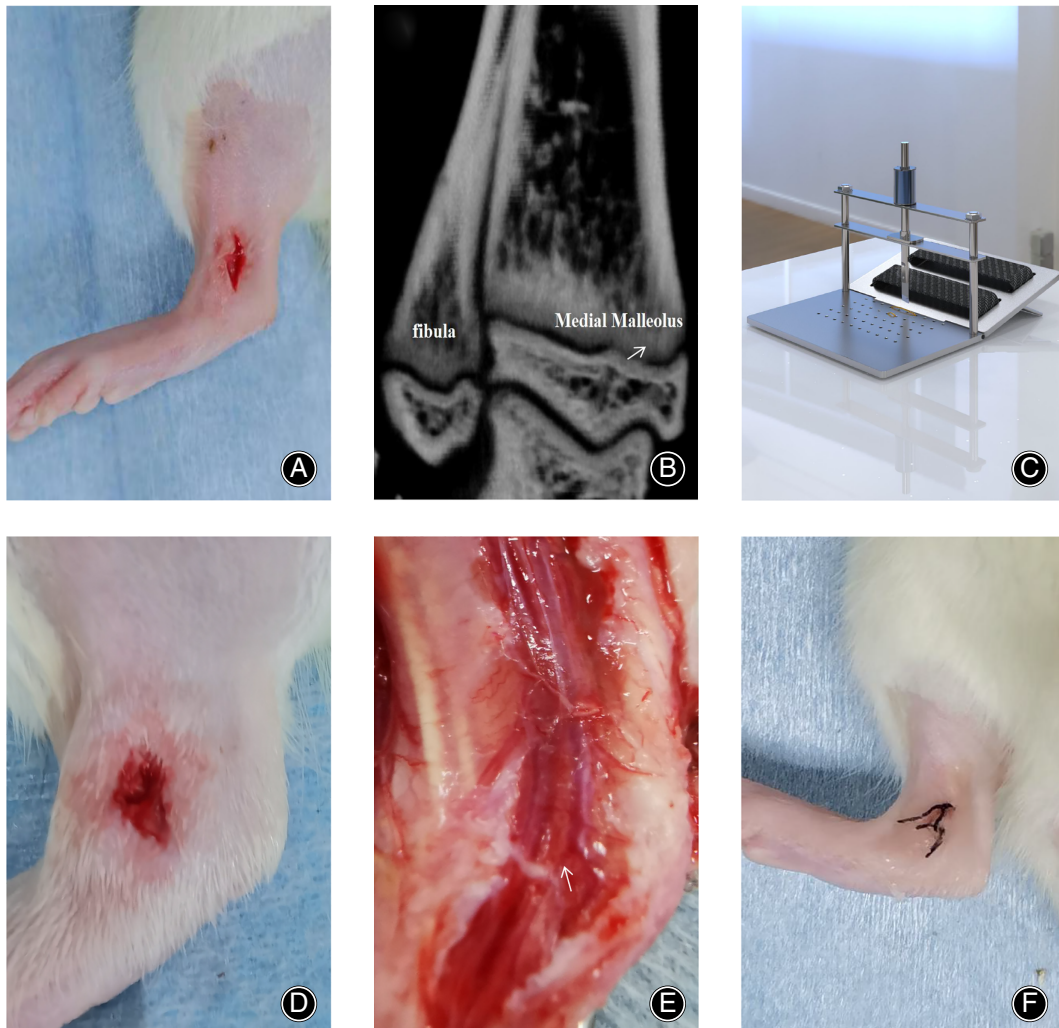A RAT MODEL OF ANKLE FRACTURE WITH VASCULAR INJURY

Fig. 2 Establishment of a rat medial malleolus fracture model. (A) After shaving and sterilization, a 1 cm incision passing through the molding equipment was made. (B) Ankle structure diagram; the white arrow indicates the medial malleolus. (C) Design drawing of the molding instrument. (D) A breach (2 mm in wide) was cut from the inferomedial aspect of the ankle end toward the central medial malleolus. (E) The saphenous artery is shown by a white arrow. (F) A wound has been sewn up after the operation in Fracture + Vascular group.

were stained for 30 min in a wet box in the dark. Then, the cell nuclei were stained with hematoxylin after washing thoroughly, and the sections were incubated at 37°C in an oven. The samples were observed under an Olympus light microscope (40×) after being sealed with neutral balsam on slides. The number of osteoblasts (OB) per unit area of each ALP staining scanning film was counted by ImageJ software (Java 1.6.0; National Institutes of Health, Bethesda, MD, USA). The experiment was repeated three times for each group, and the average value was taken. The cytoplasm of the OBs contained gray–black particles or massive, strip-shaped precipitates.

Immunohistochemistry and Immunofluorescence
To evaluate the number of capillaries in each group, the bone samples were stained for CD31 immunohistochemistry and CD34 immunofluorescence. For immunohistochemical evaluation, the expression of CD31 was detected according to the following procedure. Paraffin sections were dewaxed, hydrated, and subjected to antigen retrieval. Endogenous peroxidase activity was blocked by incubation with 3% hydrogen peroxide for 20 min, followed by incubation with 10% goat serum for 10 min. Sections were then incubated with the optimal concentration of CD31 primary antibody (1:500; Abcam, Cambridge, MA, USA) overnight at 4°C. The next day, after washing three times with PBS, the slides were incubated with secondary antibody (1:2000; Abcam, Cambridge, MA, USA) for 45 min. Subsequently, the slides were visualized using diaminobenzidine (DAB). The nuclei were counterstained with hematoxylin. The slides were visualized with an optical light microscope (Olympus BX51TR, Tokyo, Japan). Brown-colored cells were considered positive for the antigen.

The simple experimental procedure for CD34 immunofluorescence staining is as follows. Deparaffinized sections were washed with PBS for antigen retrieval. The sections were blocked with 10% donkey serum for 30 min at room temperature, washed extensively and then incubated with CD34 primary antibody working solution overnight at 4°C. The next day, after washing three times with PBS, the slides were incubated with Alexa Fluor® 488 donkey anti-rabbit IgG (H + L) antibody for 45 min. After washing, nuclei were stained with 4,6-diamino-2-phenylindole (DAPI, 1:500) and incubated in the dark for 5 min. After blocking with an anti-fluorescence quencher, they were observed under the fluorescence microscope (Olympus BX51TR, Tokyo, Japan). Five high-power microscope fields were randomly selected to observe and take pictures, and ImageJ was used to count the number of CD34-positive cells. Each experiment was repeated three times, and the average value was taken.

Statistical Analysis

All parameters in the experimental and control lateral medial malleoli were quantitatively compared using SPSS 19.0 software (IBM Corp., Armonk, NY, USA). They include the growth rate of blood flow perfusion, percentage of OBs and OCs in histologically determined ROIs, and the number of neovascular endothelial cells represented by CD31 and CD34. For comparisons between multiple groups, one-way analysis of variance (ANOVA) and Tukey's postmortem multiple comparison test were used. A $P < 0.05$ was considered statistically significant.

Results

Each animal showed good mental status and ate regularly after surgery. The operative wounds healed on time, with no evidence of sudation or maturation. All animals could walk slowly for 4 h after the operation. None of the animals died suddenly or became bedridden throughout the study period.

Micro-CT Scan

Mesial coronal section images of micro-CT scans showed (Fig. 3) that, compared with the normal medial malleolus (Figs 3A,D), the medial malleolus was destroyed in the Fracture group (Fig. 3B) and Fracture + Vascular group (Fig. 3C). The medial malleolus healed in the F group (Fig. 3E), but there was no significant healing in the Fracture + Vascular group (Fig. 3F) after 6 weeks.

Laser Doppler Flowmetry Scanning

The blood flow of the medial malleolus in each group was measured by LDF. The results showed that the average blood perfusion of the medial malleolus in the Sham group was approximately 50, while that of the medial malleolus in the
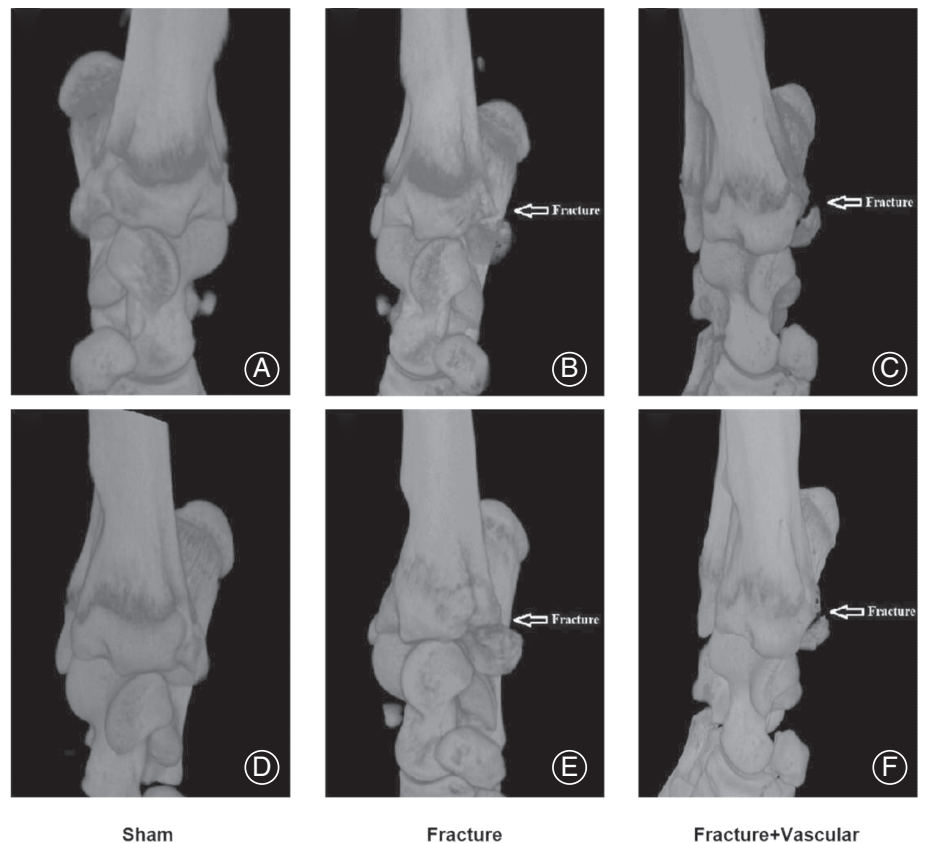
Fig. 3 Micro-CT images of the medial malleolus of rats in each group. (A and D) are micro-CT images of a normal medial malleolus. (B) is a micro-CT image of the rat in the Fracture group after 24 h. (C) is a micro-CT image of the rat in the Fracture + Vascular group after 24 h. (E) is a micro-CT image of the rat in the Fracture group after 6 weeks. (F) is a micro-CT image of the rat in the Fracture + Vascular group after 6 weeks.
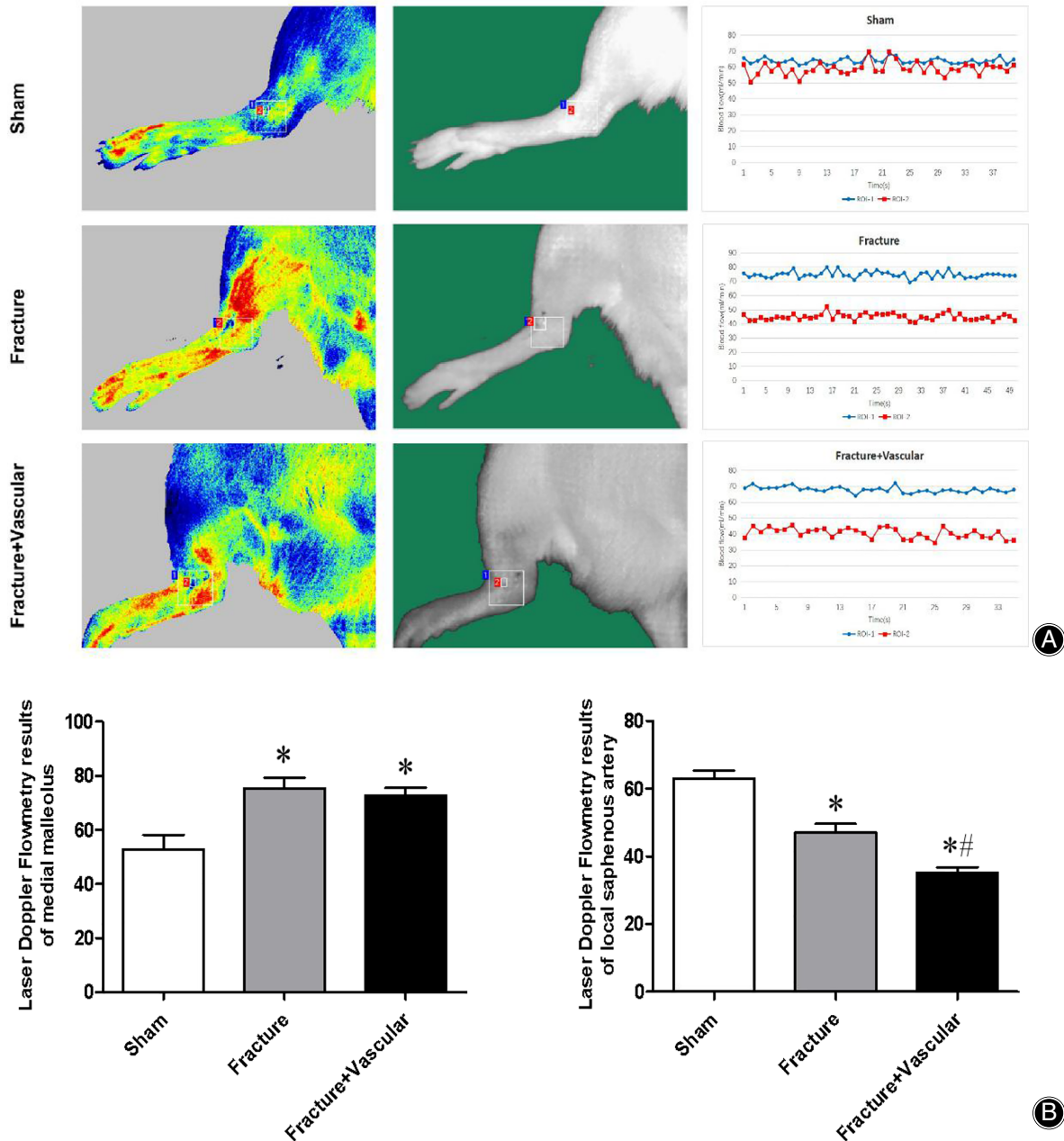
Sham   Fracture   Fracture+Vascular

Fig. 4 Blood perfusion volume of rats in each group. (A) laser doppler flowmetry (LDF) scanning test results. (B) LDF statistical results for each group. $n = 6$. The data are the mean $\pm$ SEM. Compared with the Sham group, $*P < 0.05$; compared with the Fracture group, $^{\#}P < 0.05$.

fracture group was increased significantly relative to the Sham group after 24 h ($P < 0.05$). The average blood perfusion of the medial malleolus in the vascular injury group was 75, an increase by approximately 50% relative to the Sham group, with which it was also significantly higher ($P < 0.05$). In the area of the local saphenous artery, the average blood perfusion of the medial malleolus in the fracture group and the vascular injury group was significantly lower than that in the Sham group. However, the average blood perfusion in the area of the local saphenous artery in the vascular injury group was smaller and was significantly lower than that in the fracture group ($P < 0.05$). The results showed that the total blood flow of the medial malleolus increased significantly 24 h after fracture injury. The total blood flow decrease was not significant even if the saphenous artery was injured. However, the blood perfusion of the saphenous artery at the medial malleolar fracture site decreased significantly,
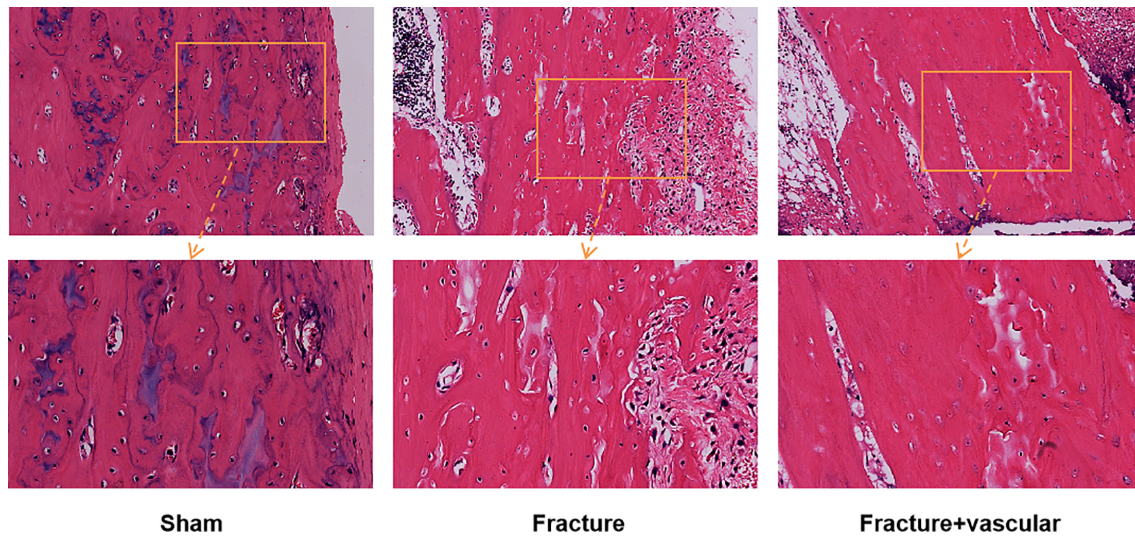
Fig. 5 Histological examination (HE) results for the fracture site in each group 24 h after fracture. $n = 6$. The number of osteocytes in the Fracture + Vascular group had significantly decreased relative to those in the Sham group and the Fracture group.

which may be the cause of the delayed fracture healing (Fig. 4).

Histological Examination
Histological examination (HE) staining showed that trabecular bone, bone cells and some cartilage tissue were seen in the Sham group. In the Fracture group, the number of trabecular bone and bone cells were reduced, and the number of osteoblasts had increased. In the Fracture + Vascular group, the number of trabecular bone and bone cells were further reduced, the cells exhibited nuclear vacuolization, and the osteoblasts had disappeared. The results indicated that vascular injury has a significant effect on the osteocytes (Fig. 5).

TRIP and ALP Examination
ALP and TRAP staining results showed that the number of OBs and OCs in the Sham group was less than that in the Fracture group, and there were a large number of OBs and OCs in the fracture site 24 h after fracture, which was statistically significant compared with that in the Sham group. The experimental results also showed that the number of OBs and OCs in the fracture site of the Fracture + Vascular group decreased significantly 24 h after fracture, which was significantly different from that of the Fracture group (Fig. 6).

Immunohistochemistry and Immunofluorescence
It was found that the number of neovessels in the Sham group was significantly lower than that of the Fracture group through CD31 immunohistochemistry and CD34 immunofluorescence staining experiments. After 24 h of vascular injury, the number of neovessels in the Fracture + Vascular group had decreased significantly relative to that in the Fracture group. This

phenomenon indicates that vascular damage may affect the local blood supply and capillary regeneration of fractures, thereby affecting the fracture rehabilitation process (Fig. 7).

Discussion
In this paper, a rat model of ankle non-union was established by fracture surgery with vascular injury. The fracture model was stable and reliable through a variety of experimental methods.

Animal Models
Basic and clinical research on medial malleolar fractures has recently become a popular topic in the field of foot and ankle surgery, but progress has been slow. Development of a reproducible fracture animal model appeared to be an insurmountable bottleneck for studying medial malleolar fractures. To solve this problem, a homemade medial malleolar fracture tool was developed by our research group and was used to establish a repeatable and stable rat model, which provides a solid foundation for the study of medial malleolar atrophic non-union.

Numerous studies have reported fracture non-union models. Hietaniemi et al.[20] reported non-union modeling, but their modeling method lacks repeatability and stability and does not consider factors important for vascular injury; therefore, it cannot perfectly address the problem of medial malleolar fracture healing.[21] Our research group deeply studied the anatomical structure of the ankle joint of rats and developed customized ankle joint tools. The tools ensure that the bone knife and the long axis of the long bone maintain a 37° angle, the force exerted by the bone knife can be controlled, the ankle bone of animals can be firmly fixed, and consistency can be guaranteed. To confirm the repeatability and stability of the model, we used micro-CT scanning to collect images of the
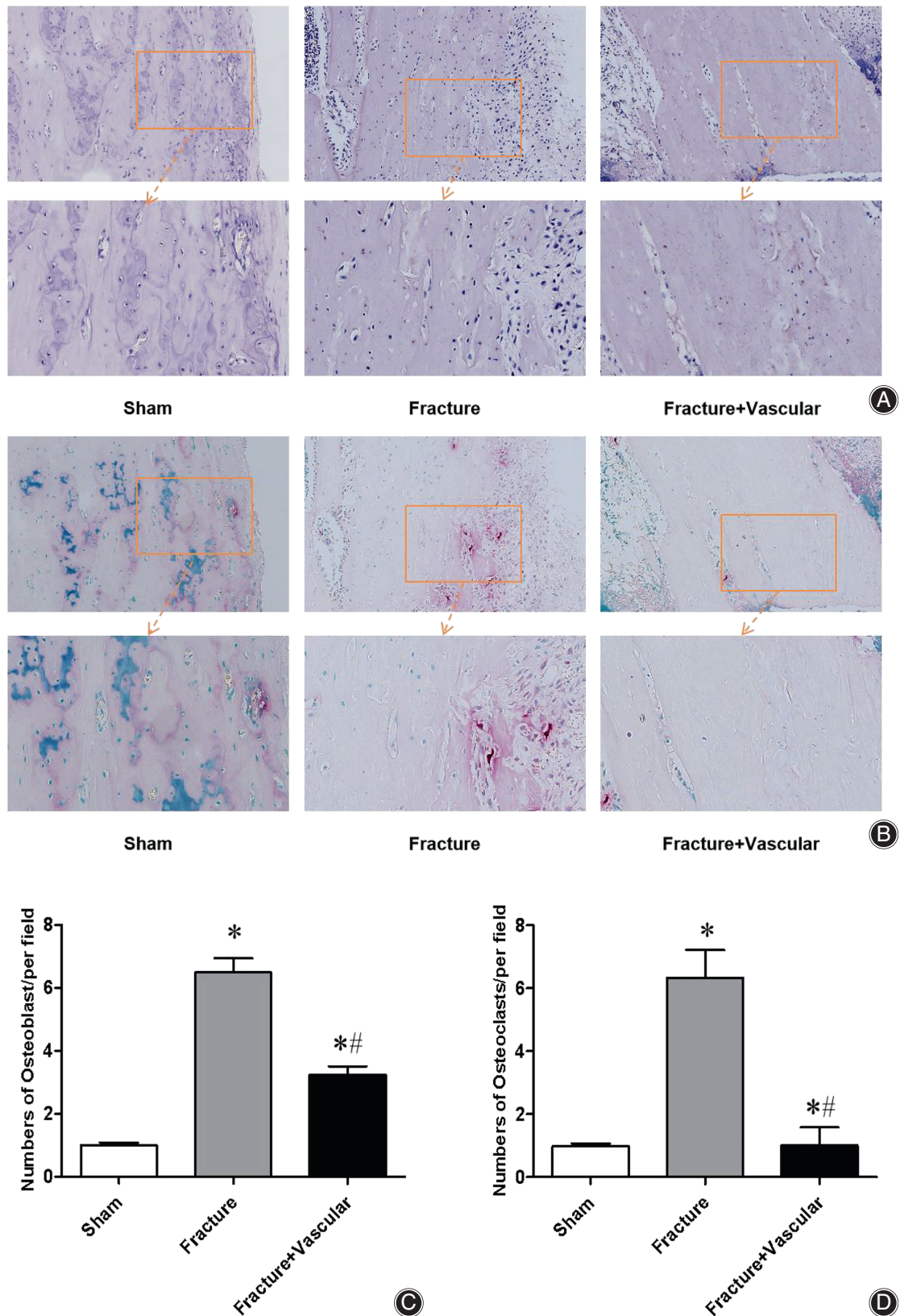
Fig. 6 Number of osteoblasts (OBs) at the fracture site. (A) ALP staining results of the fracture site in each group. (B) The results of TRAP staining of the fracture site in each group. (C) Statistical results for the OBs in each group. (D) Statistical results for the OCs in each group. $n = 6$. The data are the mean $\pm$ SEM. Compared with the Sham group, $*P < 0.05$; Compared with the Fracture group, $\#P < 0.05$.

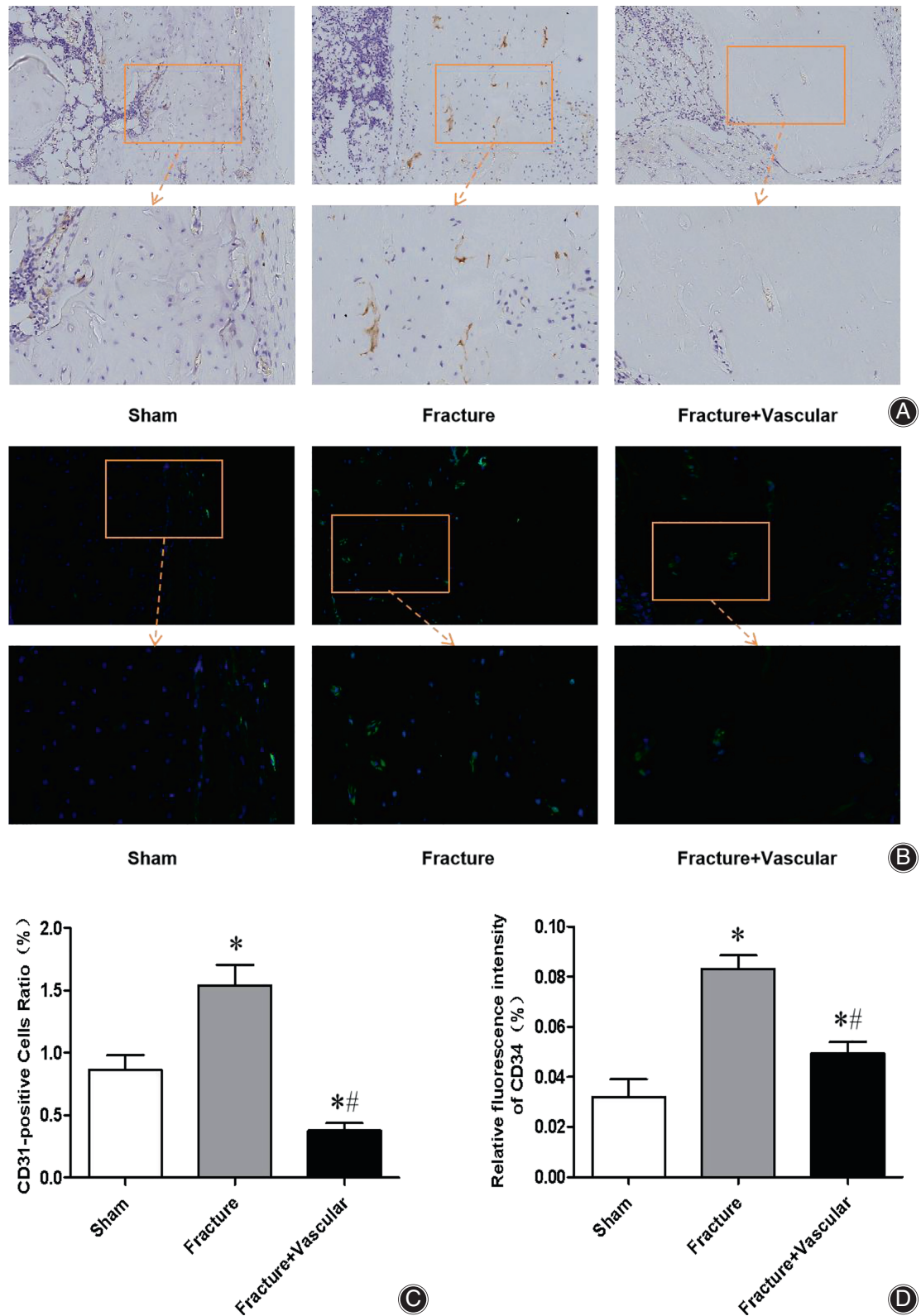A RAT MODEL OF ANKLE FRACTURE WITH VASCULAR INJURY

Fig. 7 The number of neovessels at the fracture site. (A) The results of CD31 immunohistochemistry of the fracture site in each group. (B) The results of CD34 immunofluorescence of the fracture site in each group. (C) The number of CD31-positive cells in each group was statistically analyzed. (D) The statistical results for the CD34-positive cells in each group. $n = 6$. The data are the mean $\pm$ SEM. Compared with the Sham group, *$P < 0.05$; Compared with the Fracture group, #$P < 0.05$.

medial malleolar fracture and reconstructed them in 3D. The three-dimensional reconstruction images of the micro-CT scans of the models showed that medial malleolar fracture was successfully created in the operated rats, which confirmed the high efficiency, stability and repeatability of the homemade tool.

Influence of Blood Supply

Bone is a highly vascularized tissue, and its angiogenesis is closely related to fracture healing.[17] Studies have confirmed that the total blood flow of the bone decreases immediately after fracture or osteotomy, and the blood circulation of cortical bone can be reduced by approximately 50%.[22] Both the initiation of local vascular injury and the later lack of new inward growth of blood vessels can cause a lack of blood supply in the tissue near the fracture, which easily leads to bone non-union.[17,23] To further study the effect of vascular injury on the rehabilitation of medial malleolar fractures, we created a vascular injury model based on our successful medial malleolar fracture model. A micro-CT scan showed that there was basically no new bone formation in the medial malleolus with saphenous artery amputation 6 weeks after the operation, while a large amount of new bone formation was observed in the medial malleolus without vascular injury. The experimental results confirmed the success of the model of medial malleolar fracture combined with vascular injury. Simultaneously, we also found that there was a positive correlation between blood flow perfusion and the number of OCs and OBs. It was also found that the number of vascular endothelial cells at the site of the medial malleolar fracture decreased after vascular injury. We found that arterial vascular injury had a serious impact on the formation of OCs and OBs and on neovascularization, which also confirmed the important role of vascular injury in medial malleolar fracture non-union, providing a reliable experimental basis for further basic research and clinical trials.

Limitations

In this paper, in the process of fracture group modeling, some microvessels and periosteal vessels were inevitably damaged, but the effect was not significant.

Conclusion

In this paper, we successfully developed a consistent and repeatable model of medial malleolar fracture combined with vascular injury in rats, the most common model animal used in medicine. The model can be used for the study of the effect of vascular injury on medial malleolar fracture injury and establishes a good foundation for the study of ankle non-union.

Author Contributions

Sun Jinglai, Li Zhigang and Yu Hui conceived and designed the whole research. Liu Chong and Sun Jinglai conducted experiments. Li Qifeng and Yu Hui contributed analytical tools. YM, WS and SJ analyzed data. SJ and LC wrote the manuscript. WG, ZJ and LH edited the manuscript. All authors read and approved the manuscript.

Ethical Approval

All procedures performed in studies involving human participants were in accordance with the ethical standards of the institutional and/or national research committee and with the 1964 Helsinki declaration and its later amendments or comparable ethical standards.

References

1. Fisher N, Atanda A, Swensen S, Egol KA. Repair of bimalleolar ankle fracture. J Orthop Trauma. 2017;31:S14–5.
2. Winge R, Bayer L, Gottlieb H, Ryge C. Compression therapy after ankle fracture surgery: a systematic review. Eur J Trauma Emerg Surg. 2017;43: 451–9.
3. Sparks DS, Saifzadeh S, Savi FM, Dlaska CE, Berner A, Henkel J, et al. A preclinical large-animal model for the assessment of critical-size load-bearing bone defect reconstruction. Nat Protoc. 2020;15:877–924.
4. Frolke JP, Patka P. Definition and classification of fracture non-unions. Injury. 2007;38(Suppl 2):S19–22.
5. Hak DJ, Fitzpatrick D, Bishop JA, Marsh JL, Tilp S, Schnettler R, et al. Delayed union and nonunions: epidemiology, clinical issues, and financial aspects. Injury. 2014;45(Suppl 2):S3–7.
6. Wu XQ, Wang D, Liu Y, Zhou JL. Development of a tibial experimental non-union model in rats. J Orthop Surg Res. 2021;16:261.
7. Liu J, Zhang L, Tang P. Diagnosis and treatment of fracture delayed union and non-union. Zhonghua Wai Ke Za Zhi. 2015;53:464–7.
8. Zhang L, Jiao GJ, Ren SW, Zhang X, Li C, Wu W, et al. Exosomes from bone marrow mesenchymal stem cells enhance fracture healing through the promotion of osteogenesis and angiogenesis in a rat model of non-union. Stem Cell Res Ther. 2020;11:38.
9. Park SH, Silva M, Bahk WJ, McKellop H, Lieberman JR. Effect of repeated irrigation and debridement on fracture healing in an animal model. J Orthop Res. 2002;20:1197–204.
10. Brownlow HC, Simpson AH. Metabolic activity of a new atrophic non-union model in rabbits. J Orthop Res. 2000;18:438–42.
11. Kokubu T, Hak DJ, Hazelwood SJ, Reddi AH. Development of an atrophic non-union model and comparison to a closed healing fracture in rat femur. J Orthop Res. 2003;21:503–10.
12. Kaspar K, Matziolis G, Strube P, Sentürk U, Dormann S, Bail HJ, et al. A new animal model for bone atrophic non-union: fixation by external fixator. J Orthop Res. 2008;26:1649–55.

13. Okanobo H, Khurana B, Sheehan S, Duran-Menditcuti A, Arianjam A, Ledbetter S. Simplified diagnostic algorithm for Lauge-Hansen classification of ankle injuries. Radiographics. 2012;32:71–84.
14. Kular J, Tickner J, Chim SM, Xu J. An overview of the regulation of bone remodelling at the cellular level. Clin Biochem. 2012;45:863–73.
15. Large TM, Adams MR, Loeffler BJ, Gardner MJ. Posttraumatic avascular necrosis after proximal femur, proximal humerus, talar neck, and scaphoid fractures. J Am Acad Orthop Surg. 2019;27:794–805.
16. Tong XY, Chen X, Zhang SH, Huang M, Shen X, Xu J, et al. The effect of exercise on the prevention of osteoporosis and bone angiogenesis. Biomed Res Int. 2019;2019:8171897.
17. Kusumbe AP, Ramasamy SK, Adams RH. Coupling of angiogenesis and osteogenesis by a specific vessel subtype in bone. Nature. 2014;507: 323–8.
18. Hu DP, Ferro F, Yang F, Taylor AJ, Chang W, Miclau T, et al. Cartilage to bone transformation during fracture healing is coordinated by the invading vasculature and induction of the core pluripotency genes. Development. 2017;144:221–34.
19. Fraser LA, Papaioannou A, Adachi JD, Ma JH, Thabane L, Group CR. Fractures are increased and bisphosphonate use decreased in individuals with insulin-dependent diabetes: a 10 year cohort study. BMC Musculoskelet Disord. 2014;15:201.
20. Hietaniemi K, Peltonen J, Paavolainen P. An experimental model for non-union in rats. Injury. 1995;26:681–6.
21. Liang DW, Sun J, Wei FY, Zhang J, Li P, Xu Y, et al. Establishment of rat ankle post-traumatic osteoarthritis model induced by malleolus fracture. BMC Musculoskelet Disord. 2017;18:464.
22. Kelly PJ, Montgomery RJ, Bronk JT. Reaction of the circulatory system to injury and regeneration. Clin Orthop Relat Res. 1990;254:275–88.
23. Murnaghan M, Li G, Marsh DR. Nonsteroidal anti-inflammatory drug-induced fracture non-union: an inhibition of angiogenesis? J Bone Joint Surg Am. 2006; 88:140–7.